PHYSICAL REVIEW B VOLUME 5, NUMBER 6 15 MARCH 1972

X-Ray-Photoelectron Spectrum of Diamond

Thaddeus Gora, Ralph Staley,* J. D. Rimstidt, and J. Sharma
Solid State Branch, Feltman Research Laboratory, Picatinny Arsenal, Dover, New Jersey 07801

(Received 1 November 1971)

The x-ray-photoelectron spectrum of powdered diamond samples in the binding-energy range −15 to 1050 eV is reported. The major features of the spectrum are the C 1*s* and surface contaminant O 1*s* peaks, the carbon and oxygen Auger transitions, and diamond's valence-region structure. Plasma-resonance excitations are identified in the inelastic tail of the C 1*s* peak. The valence-region spectrum is analyzed and corrected for the presence of what is interpreted to be extrinsic structure. The corrected spectrum maps out primarily the *s*-like states in diamond's density of states, and indicates a valence-band width of 21 eV.

I. INTRODUCTION

X-ray-photoelectron spectroscopy (XPS) provides a ready method to map some major features of the occupied electronic structure of solids.[1] The theoretical framework appropriate to extract the most information from this mapping varies with the type of material studied. But many aspects of the interpretation of the experimental data and its comparison with theory are common to studies of similar materials.[2]

This paper examines the application of the XPS experiment to diamond, a simple covalent insulator. Diamond proves to be an interesting choice for XPS study for several reasons: Characteristic energy-loss data is available from electron-scattering experiments[3]; this aids in and reinforces the interpretation of the inelastic tail structures which are associated with the primary peaks. Several calculations are available giving predictions of the width and internal structure of the valence band[4–12]; the comparison of the experimental results to these predictions is instructive. Finally the application of a new technique to a simple and long-studied material helps to put both the strengths and weaknesses of the technique in perspective.

II. EXPERIMENTAL

The instrument used in these experiments was a Varian IEE-15 spectrometer. Preliminary studies were done using a powdered sample of diamond supplied by the National Bureau of Standards. This was mounted by attaching Scotch tape to the sample cylinder sticky side out and rolling this in the diamond powder. Previous investigations indicate that powders mounted in this way will completely cover the substrate. More extensive studies were made using samples of type-I, type-IIa, and type-IIb diamond powders provided by Dyer and Caveney of the DeBeers Diamond Research Laboratory. These were prepared by crushing previously characterized single crystals of diamond in a ball mill. Preliminary cleaning in nitric acid was found to leave traces of tungsten so that final cleaning in a solution of equal parts of nitric and hydrofluoric acids was required. Some selection for particle size was made by a decanting step in the cleaning process which removed the suspended (smaller) particles. Microscopic examination of the mounted sample showed that the exposed surfaces consisted almost entirely of faces of 100 μ or more. These samples were all mounted as described above.

All spectra were obtained using a magnesium anode. A vacuum of 2×10^{-7} torr was obtained but the sample surfaces were not specially cleaned of adsorbed gases or carbon contaminants. Run times ranged from 5 min for 12-eV (120-data-channel) scans of core lines to 60 h for 100-eV (500-data-channel) scans of the valence-band region.

III. RESULTS

Identification of the nature of XPS lines is facilitated by the use of tables of core lines for the elements.[1,13] The exact values for line positions, however, depend on the choice of a zero of binding energy. The experimental zero read by the Varian instrument has been arbitrarily retained without corrections. Calibrations for charging effects are possible to within a few tenths of an eV. But the zero obtained, the surface Fermi level of the sample under the experimental conditions, is not meaningful. It cannot in practice be related to the band structure (the edge of the valence or conduction band or the vacuum level) with an uncertainty of less than half the band gap.[14] For wide band gap materials such as diamond this uncertainty amounts to several eV. The use of the term "calibration" to describe the corrections for charging which are commonly made has been unfortunate since a meaningful zero is not obtained. In the case of diamond it would not be reliable to better than about ±4 eV. Comparison of the C 1*s*, O 1*s*, and apparent valence-band edge positions with those in graphite assures us that the zero for our diamond spectrum has not wandered by as much as 4 eV. Graphite, being a conductor, does have a well-defined zero

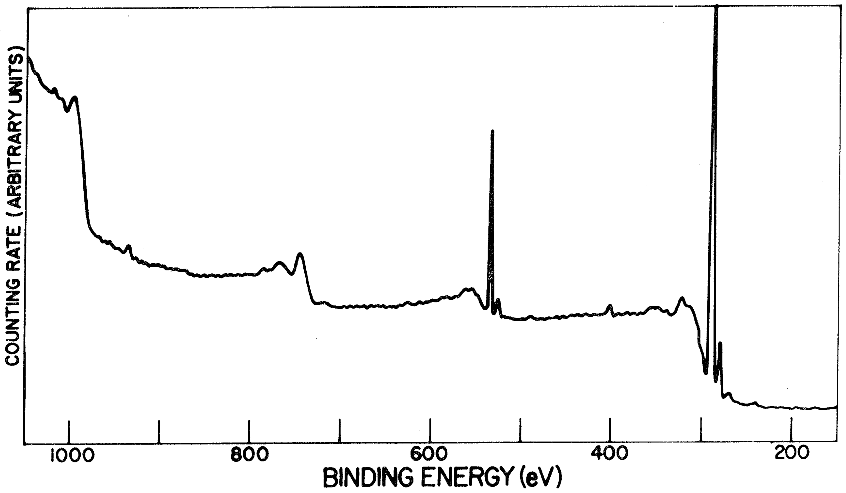

FIG. 1. XPS spectrum of a diamond sample in the core-level region.

of binding energy.

The spectrum obtained for one of our samples in the binding-energy range 150–1050 eV is shown in Fig. 1. Spectra in this energy range are essentially identical for all our samples of diamond. The peak at 287 eV is due to the only true diamond core level, the C 1*s* level. The smaller peak directly to its right is produced by the Mg $K\alpha_{3,4}$ component in the x radiation and is a reproduction of the C 1*s* peak. The primary peak arises from the Mg $K\alpha_{1,2}$ component, and its observed width of 1.65 eV is due to the combined effects of the x-ray linewidth (0.7 eV) and the instrument resolution (1.0 eV). The other prominent peak in Fig. 1, at 533 eV, is the O 1*s* line due to oxygen or oxide surface contamination. Both the C 1*s* and O 1*s* lines have structures to the higher-binding-energy side of the main peaks. We shall refer to these structures as their inelastic tails. In Fig. 2 the primary peaks of the C 1*s* and O 1*s* lines have been superposed to facilitate comparison of their inelastic tails. Returning to the spectrum of Fig. 1, the structures at 745 and 1000 eV are due to oxygen and carbon Auger transitions, respectively. Finally, the presence of a small peak at 400-eV binding energy due to the N 1*s* level indicates that that sample contains of the order of 1% nitrogen. Nitrogen-impurity content of this order is commonly found in type-I diamond.

Figure 3 shows the spectrum in the valence region up to 40-eV binding energy. The steep rise in base line across this range which partly obscures the spectrum results from the cumulative effects of the inelastic tail structures of the underlying primary

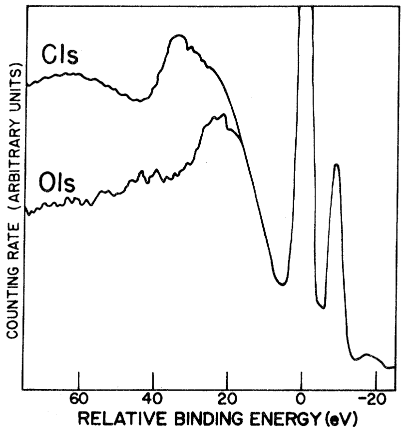

FIG. 2. Inelastic tails of the C 1*s* and O 1*s* peaks in the photoelectron spectrum of a diamond sample. Relative binding energy is measured with respect to the centers of the primary XPS peaks, and the vertical scale has been adjusted to superpose these peaks.

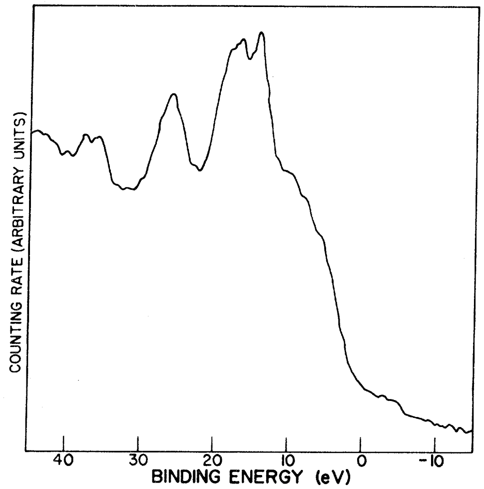

FIG. 3. XPS spectrum of a diamond sample in the valence-level region.

spectrum. X-ray satellite contributions are also present.

The remaining region of the spectrum, 45–150 eV, contained a variety of weak peaks. One of these, at 54 eV, reproduces the C 1*s* line at 287 eV because of the presence of Al $K\alpha_{1,2}$ radiation arising from aluminum contamination of the x-ray anode. Other peaks in this region are not so readily explained. Most of these peaks, however, occurred in the spectrum of only one of the samples of diamond studied. In one sample, peaks occurred at 76, 102, 119, and 124 eV, and in another at 65, 140, and 146 eV. Although we have no totally satisfactory explanation for their occurrence, they may be due to bulk or surface-impurity species. In any case, we believe they can be discounted as intrinsic peaks of the diamond spectrum.

IV. DISCUSSION

In XPS experiments, x rays are absorbed by a sample with the emission of photoelectrons, and the kinetic-energy distribution of the electrons ejected from the sample is recorded. The observed spectrum should be a map of the energy distribution of bound electrons in the sample. But the map is modulated in several important ways. It reflects not only the density of states at a given energy but also the XPS cross section, the transition probability from bound states to detectable free states. This cross section is a function of orbital symmetry as well as energy. Also, the observed spectrum contains several superimposed reproductions of the map since the x-ray source produces not only the Mg $K\alpha_{1,2}$ line but also several "satellite" lines. And finally, scattering of the primary electrons, the emission of secondary electrons, and instrumental contributions produce a structured background in the observed spectra. In our analysis of the spectra, each of these points will receive further attention.

A. Inelastic Tails

The inelastic tails of the C 1*s* and O 1*s* lines in the diamond spectrum (Fig. 2) merit special attention. The C 1*s* tail is nearly identical to the spectrum obtained by Whetten[3] by reflecting a monoenergetic electron beam from clean (treated in H_2 at 700 °C) diamond surfaces. Whetten identified the structure in his spectrum as resulting from a plasma-resonance energy-loss process peaking at 31 eV. This corresponds to the first peak in our C 1*s* tail at 34 eV. The second peak at 63 eV arises from electrons which have twice undergone plasma-resonance energy loss.

For both Whetten's experiment on clean surfaces and our C 1*s* tail, the majority of electrons detected have traveled some distance through the diamond itself. In the XPS case the sampling depth is only about 100 Å. For Whetten's experiment the depth should be about half of this. The electron kinetic energy used was 1150 eV (a bit larger than the 967 eV for C 1*s* photoelectrons) but the beam is attenuated both on its way into and on its way out of the sample. When Whetten performed his experiments on dirty surfaces he obtained a different spectrum, one much more closely resembling the inelastic tail we obtain for O 1*s*. This is reasonable since in both cases the observed electrons mostly originate in the surface contaminant layers. They thus reflect loss processes characteristic of these layers rather than of the diamond bulk. In Whetten's experiment the shallower sampling depth allowed the surface layers to dominate. In the present O 1*s* inelastic tail region the electron source oxygen is present only in the surface layers.

These results and analysis of the inelastic tails are of interest for several reasons. They illustrate the utility of XPS for studying electron-energy-loss phenomena. They identify a specific mechanism which results in the production of structure in the inelastic tails. And they emphasize the potential sensitivity of the XPS technique for the study of surface conditions. Moreover, they favor interpreting our spectra in terms of photoelectrons largely characteristic of the diamond bulk.

B. Valence Band

Prior to any interpretation of valence-band data it is useful to make corrections for the distortions in mapping the density of states which are introduced by the XPS experiment. The C 1*s* core line is used as a model for the inelastic tail and satellite contributions to the spectrum of a discrete state. We made corrections to the observed valence-band spectrum of Fig. 3 by use of a computer program written here. Details of a correction procedure have been given by Fadley and Shirley.[15] The corrected spectrum, Fig. 4 (solid curve), has lost some minor spurious peaks and has a level base line allowing a better look at the shape of the valence band.

The width and shape of the observed valence-band structure may be compared with theory. Several calculations have been done giving predictions of the width of the diamond valence band (Table I). Because the derivative of the density of states is discontinuous at a band edge, the points of maximum change of derivative in the high- and low-energy tails of the valence-band spectrum should be taken as the band edges. For the spectrum in Fig. 4 (solid curve) the structure between 33 and 40 eV should be disregarded. It showed substantial intensity variation from one sample to another and thus may be identified as not intrinsic in origin. A determination of the width of the remaining structure by the criterion given above yields a value of 30 eV.

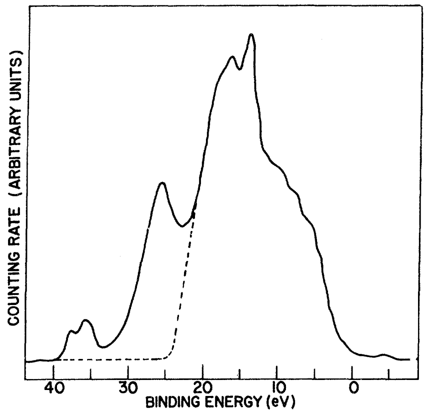

FIG. 4. Corrected valence-region spectrum for diamond. Contributions from inelastic scattering and x-ray satellites have been subtracted out. Dashed curve indicates spectrum when structure thought to be extrinsic is discounted.

This is in the top end of the range of predicted values.

A difficulty with the results obtained here is that surface states may well be a major contributor to the observed valence-band spectrum. The core O 1*s* line is one-third as strong as the core C 1*s* line. Since the XPS cross section for O 1*s* is twice that for C 1*s*, this implies that one-sixth of the atoms sampled are oxygen. If the ratio of oxygen to carbon cross section for the valence states is between 1 and 2, then from one-sixth to one-third of the observed valence-band structure is due to oxygen.

It is in fact very likely that the oxygen contamination entirely accounts for the peak centered near 25 eV in the valence-band spectrum (Fig. 4). The spectra of several simple oxygen-containing compounds indicate that the O 2*s* electrons can be expected to occupy a localized state which falls near 25 eV in solid samples.[16] Lines falling at this point in the spectra of several other solids lend further support to this conclusion.[17] Because of the large amount of oxygen contamination and the evidence that most of the oxygen valence-band intensity should fall between 20 and 30 eV, most of the intensity in the 20–30-eV range will be assumed to be due to states of the surface oxygen. Accordingly, using the left half of the 25-eV peak as a model, a symmetric peak of that shape was constructed and substracted from the valence-band spectrum (Fig. 4). The result is shown in Fig. 4 (dashed curve).

TABLE I. Calculated valence-band widths in eV.

Kleinman *et al.* (1962)[a]	21.9
Stocker (1962)[b]	14.7
Cohan *et al.* (1963)[c]	25.2
Bassani *et al.* (1963)[d]	23.2
Keown (1966)[e]	19.6
Herman *et al.* (1966)[f]	21.2
Saslow *et al.* (1966)[g]	28.0
Hemstreet *et al.* (1970)[h]	28.8
Pugh (1970)[i]	31.6

[a] Reference 4.
[b] Reference 5.
[c] Reference 6.
[d] Reference 7.
[e] Reference 8.
[f] Reference 9.
[g] Reference 10.
[h] Reference 11.
[i] Reference 12.

The bandwidth obtained from this corrected spectrum, about 21 eV, agrees most closely with Herman's prediction[9] for the width of the diamond valence band (Table I). The structure remaining in the valence-band region may still in part arise from states of the oxygen contaminants or other extrinsic and intrinsic surface states. But it seems reasonable to believe that the over-all shape of the dashed spectrum in Fig. 4 is correct. This may be compared with theory.

A prediction of the shape of the diamond valence-band density of states is possible. We note first that Herman's valence-band structure for diamond[9] differs from that for germanium[18] mainly by an over-all energy scaling. The detailed calculation for the density of states of germanium by Herman[18] was therefore tailored for diamond by scaling the width appropriately. A Lorentzian line shape of 1.65-eV full width at half-height was used to broaden the calculated band shape for comparison to the spectrum. This line shape was chosen to approximate the observed experimental broadening of the C 1*s* core line. The results are shown in Fig. 5 for a bandwidth of 21 eV. The lack of agreement in the comparison of this prediction with the corrected spectrum (dashed curve, Fig. 4) is to be expected.

Neither the broadened theoretical density of states nor the corrections to the experimental results have included the effect of the XPS cross

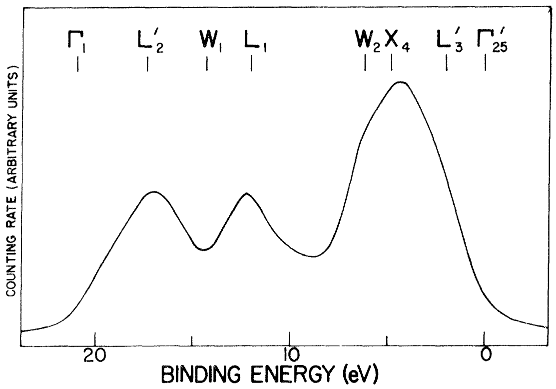

FIG. 5. Theoretical density of states for diamond's valence band, deduced from Herman's calculations (Refs. 9, 18), and Lorentzian broadened for comparison to XPS results.

sections. For carbon this effect should be substantial. We have calculated the C 2s to C 2p intensity ratio per electron for the ground state of a carbon atom to be 22 for Mg irradiation.[19] The spectra obtained by Siegbahn for simple carbon-containing species confirm that the 2s states are about an order of magnitude more intense than the 2p states for carbon.[16,20] We thus expect that those parts of the Brillouin zone with large s-like character will dominate the XPS spectrum of diamond. From the nature of the wave functions along the principal symmetry axes,[21] it is clear that the top of the valence band (especially Γ'_{25} to X_4) is dominantly p-like and that the s character is concentrated near the bottom of the band. Keeping this in mind, a comparison of the corrected experimental spectrum (dashed curve, Fig. 4) with Herman's density of states suggests that this is about right: The large peak at 4 eV in Herman's results is substantially reduced since it consists mainly of p-like states. And, the high density at the lower end of the observed spectrum is consistent with the expectation that the s character will be concentrated near the bottom of the band.

Whereas our results emphasize the s-like states in diamond's valence band, an experimental density of p-like states has for some time been available. Chalklin[22] has studied the emission of very soft x rays corresponding to transitions from the valence band to the C 1s level. The usual selection rules, plus the relative sharpness of the C 1s level, enabled him to deduce the density of p-like states. These states are primarily concentrated in a band about 10 eV wide, at the top of the valence band.

V. SUMMARY AND CONCLUSIONS

This work has identified structure in the inelastic elastic-scattering tail of diamond's C 1s peak as being due to bulk-plasma-resonance excitation. The valence-region spectrum was analyzed and corrected for what was interpreted to be extrinsic structure. The corrected spectrum maps out primarily the s-like states in diamond's valence-band density of states, and indicates a valence-band width of 21 eV.

Our experience with diamond suggests several conclusions bearing on future XPS studies of valence bands. First, surface contaminants can contribute substantially to the observed spectra. Elimination of extrinsic contaminants should be possible by use of equipment allowing heat treatment of the sample in an appropriate atmosphere or sputtering of the sample surface, and maintenance of ultrahigh vacuum. Second, available calculations giving the density of states within a valence band are not directly useful for quantitative comparison to XPS results. Each state must be weighted by its XPS cross section to correctly predict the shape of the observed spectrum. And finally, the resolution obtainable with Mg (or Al) x-ray sources and existing instruments is between 1 and 2 eV. Thus, at best, the observed spectrum is a somewhat blurred image of the XPS-cross-section-weighted density of states.

ACKNOWLEDGMENTS

We thank Dr. Frank Herman for suggesting the method we used to approximate diamond's density of states, Dr. C. Y. Fong for supplying us with a partial density of states based on his published calculation (Ref. 11), and Dr. P. J. Kemmey for helpful suggestions. We are grateful for the comments of Dr. D. Wiegand and Dr. D. S. Downs regarding the preparation of the manuscript.

---

[*] Present address: Department of Chemistry, California Institute of Technology, Pasadena, Calif. 91109.

[1] K. Siegbahn, C. Nordling, A. Fahlman, R. Nordberg, K. Hamrin, J. Hedman, G. Johansson, T. Bergmark, S. Karlsson, I. Lindgren, and B. Lindberg, *ESCA-Atomic, Molecular and Solid State Structure Studied by Means of Electron Spectroscopy* (Almqvist & Wiksells boktryckeri AB, Uppsala, Sweden, 1967).

[2] R. Staley, T. F. Gora, J. D. Rimstidt, and J. Sharma, in *Proceedings of the International Conference on Electron Spectroscopy* (North-Holland, Amsterdam, to be published).

[3] N. R. Whetten, Appl. Phys. Letters 6, 135 (1966).

[4] L. Kleinman and J. C. Phillips, Phys. Rev. 125, 819 (1962).

[5] D. Stocker, Proc. Roy. Soc. (London) A270, 397 (1962).

[6] N. V. Cohan, D. Pugh, and R. H. Tredgold, Proc. Phys. Soc. (London) 82, 65 (1963).

[7] F. Bassani and M. Yoshimine, Phys. Rev. 130, 20 (1963).

[8] R. Keown, Phys. Rev. 150, 568 (1966).

[9] F. Herman, R. L. Kortum, C. D. Kuglin, and R. A. Short, *The Physics of Semiconductors* (Physical Society of Japan, Kyoto, 1966), p. 7.

[10] W. Saslow, T. K. Bergstresser, and M. L. Cohen, Phys. Rev. Letters 16, 354 (1966).

[11] L. A Hemstreet, C. Y. Fong, and M. L. Cohen, Phys. Rev. B 2, 2054 (1970).

[12] D. Pugh, J. Phys. C 3, 47 (1970).

[13] J. A. Beardon and A. F. Burr, Rev. Mod. Phys. 39, 125 (1967).

[14] J. Sharma, R. D. Staley, J. D. Rimstidt, H. D. Fair, and T. F. Gora, Chem. Phys. Letters 9, 564 (1971).

[15] C. S. Fadley and D. A. Shirley, J. Res. Natl. Bur. Std. (U. S.) 74A, 543 (1970).

[16] K. Siegbahn, C. Nordling, G. Johansson, J. Hedman, P. F. Heden, K. Hamrin, U. Gelius, T. Bergmark, L. O. Werne, R. Manne, and Y. Baer, *ESCA Applied to Free Molecules* (North-Holland, Amsterdam, 1969), p. 40.

[17] T. F. Gora, R. H. Staley, J. D. Rimstidt, and J. Sharma, Bull. Am. Phys. Soc. 16, 636 (1971); also, unpublished results.

[18] F. Herman, R. L. Kortum, C. D. Kuglin, and J. L. Shay, in *II-VI Semiconducting Compounds*, edited by D. G. Thomas (Benjamin, New York, 1967), p. 547.

[19] T. F. Gora (unpublished).

[20] K. Hamrin, G. Johansson, U. Gelius, A. Fahlman, C. Nordling, and K. Siegbahn, Chem. Phys. Letters 1, 613 (1968).

[21] J. Callaway, *Energy Band Theory* (Academic, New York, 1964), pp. 159–160.

[22] F. C. Chalklin, Proc. Roy. Soc. (London) A194, 42 (1948).

PHYSICAL REVIEW B VOLUME 5, NUMBER 6 15 MARCH 1972

Quantum Theory of Light Scattering by Damped Polaritons

T. G. Giallorenzi
Naval Research Laboratory, Washington, D. C. 20390

(Received 12 March 1971)

A quantum-mechanical theory is developed to describe the scattering of intense laser light from polaritons. The theory includes the effects of lattice damping on the scattering process. The spectral properties of the spontaneous emission are described and the scattering intensity as a function of scattering angle is obtained. Explicit formulas for the integrated signal intensity, including the effects of finite pump-beam divergence, are derived. Difficulties previously encountered in describing the polariton dispersion curve in the presence of damping have also been resolved in the present work.

I. INTRODUCTION

In an ionic crystal, there is a strong coupling between the mechanical vibrations and electromagnetic radiation in the regions where their frequencies and wave vectors are nearly identical. This results in an excitation of the material for these energies and wave vectors which is characterized as partly photon, partly phonon in character.[1] These excitations are known as polaritons. In noncentrosymmetric crystals, these polariton modes participate in first-order Raman scattering through phonon-induced changes in the electric susceptibility and electric field-induced changes in the electric susceptibility. The study of polariton scattering of light provides useful information about certain crystal properties.[2,3] Polariton scattering also provides a means of obtaining tunable radiation in the vicinity of the transverse-optical crystal-phonon frequency.[4]

Because of the fact that in real crystals there are dissipative forces acting on the phonon modes, a complete theoretical description of the polariton scattering of light must, therefore, include the effects of damping of the lattice motion on the spectrum and magnitude of the scattered light. These dissipative forces generally arise from anharmonic coupling and/or lattice imperfections. Since there is coupling between the lattice modes and electromagnetic waves in the polariton-frequency region, the dissipation of lattice energy into heat in the crystal causes a strong attenuation of the light wave.[5] This attenuation will, of course, strongly influence the transmission and reflection of light from these crystals. In the Raman process, one generally observes the Stokes-shifted light only. When damping is included in the Raman process, quantitative differences in the character of the Stokes light arise; in particular, phonon damping leads to (a) a spectral distribution in the frequency of the scattered light, (b) a decrease in the peak intensity, and (c) a small shift in the position of the Raman line.

Benson and Mills,[6] using Green's-function techniques, were the first to consider the effect of lattice damping on Raman scattering from polariton modes. They have calculated a scattering cross section and from it have been able to predict the linewidth behavior as a function of scattering angle. Other authors have calculated the polariton dispersion curve in the presence of damping using a spatial-damping procedures.[4] This dispersion curve is, however, consistent with experiments only for small scattering angles. This procedure, i.e., the use of spatial damping (imaginary wave vector) is subject to three shortcomings[6]: (i) a lower hairpin-shaped branch which turns back when the wave number q is equal to some critical momentum q_c. It is quite clear that one cannot obtain a description of large-angle Raman scattering from transverse optical phonons using this description. (ii) When damping is large, q_c becomes quite small, and the dispersion curve turns about at very small scattering angles. (iii) For $q < q_c$, there are three distinct portions of the dispersion curve. This sug-